THE JOURNAL OF PHYSICAL CHEMISTRY C LETTERS

2008, *112,* 3−7
Published on Web 12/13/2007

Influence of the Medium Refractive Index on the Optical Properties of Single Gold Triangular Prisms on a Substrate

Carolina Novo,[†] Alison M. Funston,[†] Isabel Pastoriza-Santos,[‡] Luis M. Liz-Marzán,[‡] and Paul Mulvaney*[,†]

School of Chemistry & Bio21 Institute, University of Melbourne, Parkville, VIC., 3010 Australia, and Departamento de Quimica Fisica, Universidade de Vigo, Vigo, 36310 Vigo, Spain

Received: October 1, 2007; In Final Form: November 10, 2007

The surface plasmon resonance of small metal particles is highly sensitive to the refractive index of the surrounding medium. However, for particles dispersed on a glass surface in a polymer matrix, the effective refractive index is ill-defined. The effects of the substrate and solvent refractive indices on the surface plasmon resonance of individual gold nanoparticles (prisms and decahedra) have therefore been investigated by dark field microscopy. It is found that for any given substrate, e.g., glass or quartz, the surface plasmon band red-shifts when the solvent refractive index is increased as expected. However the sensitivity is reduced from that observed in a homogeneous medium, and the effect of the supporting polymer matrix is found to be of great importance. The effective refractive index dispersion relationship follows an equation of the form $n_{\mathrm{eff}} = (1 - \alpha)n_{\mathrm{sub}} + \alpha n_{\mathrm{med}}$ where the value of α was found to vary from 0.10 to 0.65 depending on whether the particles are embedded in a polymer matrix or deposited directly onto the substrate.

Introduction

The optical properties of colloidal metal particles are well-known to depend on the particle size, shape, electron density, and the refractive index of the surrounding medium.[1−10] Mie theory provides an exact solution for the shift in the surface plasmon resonance for an arbitrarily sized sphere in a homogeneous medium as the refractive index is varied and accurately predicts the observed color changes of gold sols in different solvents.[3,4] More recently, single nanocrystal measurements have been employed to avoid the effects of polydispersity on the measured ensemble surface plasmon resonance, allowing direct measurement of the homogeneous line width and position of the surface plasmon band of a single metal nanoparticle.[11−17] These measurements enable the importance of surface scattering and radiation damping on the line width of different shaped metal particles to be quantified.[17,18] However, for particles distributed on a glass slide and immersed in a second medium such as water or air, the effective refractive index is ill-defined and presumably lies between the values of the two media. It is important to be able to define how the effective local environment refractive index varies around a particle on a surface as the medium is altered in order to fully interpret single particle spectra. Although one can obviate this problem to some extent by the use of refractive index matching liquids, for many proposed applications of metal nanoparticles such as biosensing,[1,2,19,20] plasmonic based optical chips,[21] and SERS based single molecule detection,[22−24] it is not practical to work in such media.[25−28] Consequently, in this paper, we investigate the effects of substrate and sample preparation on the scattering properties of single gold nanoparticles, specifically the effective refractive index experienced by a nanocrystal within a polymeric film prepared by spin coating, since this is a common method of sample preparation for single semiconductor and metal nanocrystal microscopy.

Experimental Section

Materials. Ethanol, acetone, chloroform, isopropanol, toluene (reagent grade), dibromomethane (99%), and polyvinylalcohol (PVA, 80% hydrolyzed MW 8000−10 000) were all purchased from Aldrich. All chemicals were used as received. Milli-Q water was used in all preparations.

Synthesis of Gold Nanoparticles. Gold nanoparticles were synthesized by the seed-mediated growth method developed by Sanchez-Iglesias et al.[29] Briefly, gold seed particles (2-3 nm) were prepared by adding 2.5 mL of a freshly prepared 10 mM $NaBH_4$ solution to 47.5 mL of a H_2O−DMF mixture (1:18, v/v) containing 0.017 g of PVP (M_w = 10 000) and 22 μL of 0.1136 M $HAuCl_4$. The solution was stirred for 2 h and then allowed to sit for 24 h. To prepare the nanoparticles, a growth solution containing 0.825 mL of 0.1136 M aqueous $HAuCl_4$ and 15 mL of 2.5 mM PVP (M_w = 40 000) in DMF was sonicated until the band at 325 nm disappeared. The preformed seeds were then added (between 0.3 and 1.4 mL), and the resulting solution was further sonicated until complete reduction of the gold had taken place. After purification, the resulting solutions contained mainly trigonal prisms and decahedra, whereas other shapes such as octahedra and hexagonal plates were present in much smaller proportions. This colloid was used as a stock solution for sample preparation. Glass slides were cleaned by sonication in dichloromethane, then 10% NaOH, and finally with Milli-Q water.[30]

* To whom correspondence should be addressed.
[†] University of Melbourne.
[‡] Universidade de Vigo.

10.1021/jp709606u CCC: $40.75

Sample Preparation. *A. Gold Nanoparticles Completely Immersed in a PVA Film.* The stock gold nanoparticle solution was diluted by two with a 1% PVA in water solution. Samples were prepared by first spin coating clean, dry glass slides with this diluted gold nanoparticle solution (30 μL, 3000 rpm, 5 s) followed by spin coating the same slides with the 1% PVA solution in the absence of gold particles (50 μL, 3000 rpm, 5 s). The samples were allowed to dry for 5 min before being used. To measure the change in refractive index, spectra of the particles in air (on the slides) were collected first. Then a few drops of a solvent (chloroform, toluene, acetone, ethanol, isopropanol, or dibromomethane) were placed on the slides, and the spectra of the same particles were collected once more.

B. Gold Nanoparticles Partially Immersed in a PVA Film. The stock nanoparticle solution was diluted by 2 with the 1% PVA solution. The mixture was spin cast onto clean, dry glass/quartz slides (30 μL, 3000 rpm for 5 s). The samples were allowed to dry for 5 min before being used, and the measurement procedures described in A were repeated.

C. Bare Gold Nanoparticles (No PVA). The stock nanoparticle solution was diluted by 2 with water. This solution was then spin cast onto clean, dry glass, or quartz slides (30 μL, 3000 rpm, 5 s). The samples were allowed to dry 5 min before being used. The optical measurements were then carried out, as described in A.

Single Particle Spectroscopy. Spectra of individual gold nanoparticles were recorded by collecting their scattered light with a Nikon Eclipse TE-2000 microscope coupled to a Nikon Dark-field Condenser, as described elsewhere.[17] The scattered light was collected by a Nikon Plan Fluor ELWD 40×/0.60 NA objective and focused onto the entrance port of a MicroSpec 2150i imaging spectrometer coupled with a TE-cooled CCD camera (PIXIS 1024B ACTON Princeton Instruments). The spectra were integrated over 30 s. Approximately 30 spectra were collected for each solvent investigated. The raw spectra were normalized for background light by integrating over the region where the particles appear (~20 pixels on the detector) and dividing by a reference region (identical width, but with no particles).

Results

A typical image of the gold nanoparticles under dark field illumination is shown in Figure 1A. The sample contained a variety of different shapes so that the dispersion behavior of different sizes and shapes could be measured under identical illumination conditions. An electron microscope image of a typical colloid sample is presented in Figure 1B. The majority of particles are triangular prisms with canted edges and decahedra.

PVA is commonly used during spin coating to facilitate homogeneous dispersion of the particles on the substrate. The nanoparticle environments investigated are shown in Figure 2 and include samples in which the nanoparticles were (i) dispersed on glass or quartz in the absence of a PVA film, (ii) partially covered with a PVA film, which is the most commonly used sample preparation method, or (iii) completely covered with a PVA film.

The addition of PVA to the gold colloids is known to improve the optical quality of the samples considerably, producing well-dispersed, well-fixed and optically clear slides for imaging. Atomic force microscopy (AFM) was used to estimate the polymer film thickness and particle thickness after spin coating of the gold particles onto the microscope cover slips. In the absence of PVA, the particle height was found to be about 30−35 nm, in agreement with TEM and SEM measurements.[29] For particles spin coated in the presence of PVA, the measured height was consistently about 11−15 nm, indicating that the gold prisms were more than half-immersed in the PVA layer. (See representative AFM images and profile plots in Figures S1 and S2.) The scattered light spectrum of a single particle in one of the three environments outlined above was collected in air and then in the presence of a solvent with known refractive index. A list of the solvents used and their respective refractive indices measured at 21.8 °C is shown in Table 1. In all cases, the scattered light spectra of the same particle were collected in both air and the solvent, to enable a direct measurement of the refractive index induced spectral shift and to eliminate contributions due to sample polydispersity.

Examples of normalized spectra collected in air and solvent for two particles are shown in Figure 3. The shifts in surface

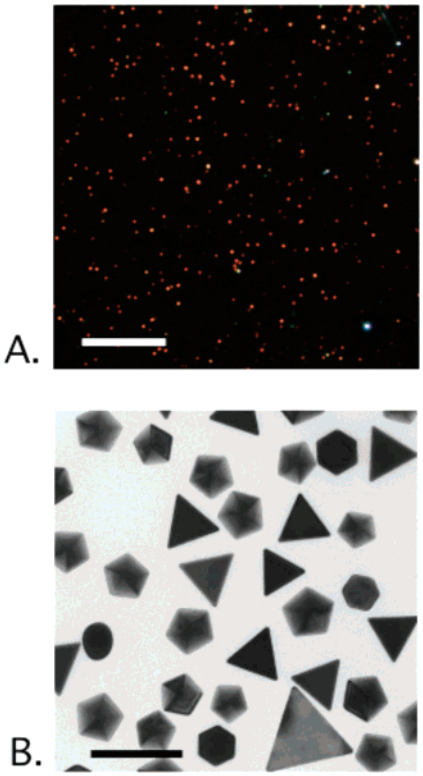

Figure 1. A. Dark field image of the gold nanoparticles (decahedra, triangles, and octahedra) in air and on glass. Scale bar = 50 μm. B. Transmission electron microscopy image of gold nanoparticles used. Scale bar = 100 nm.

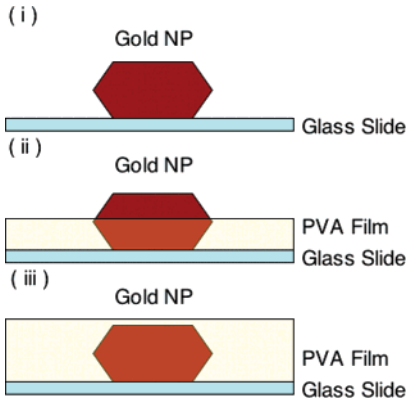

Figure 2. Systems investigated: Trigonal prisms dispersed on glass slides (i) without PVA, (ii) partially immersed, and (iii) completely immersed in a PVA film.

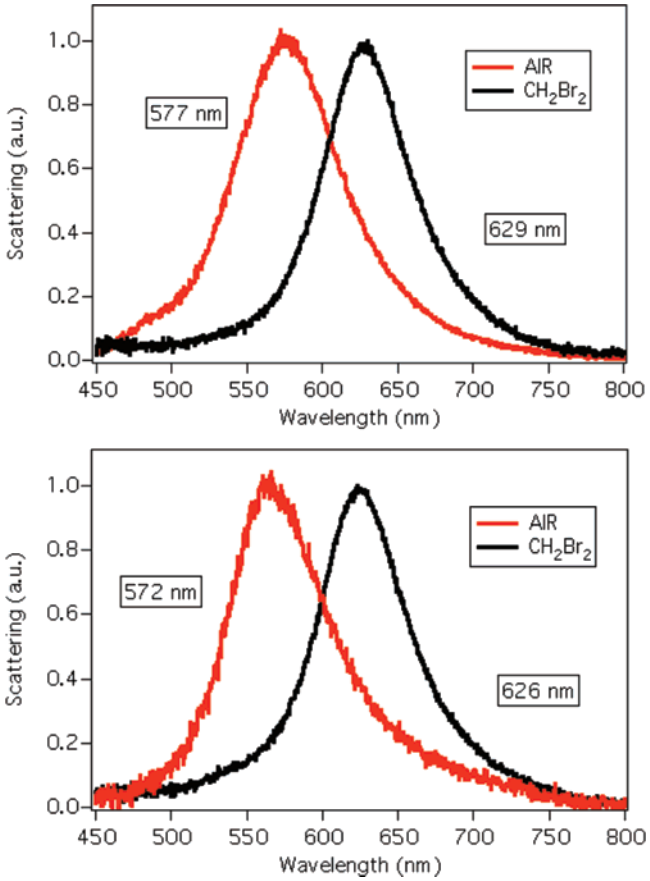

Figure 3. Normalized scattering spectra of 2 individual gold nanoparticles on glass slides (n = 1.52), in air (red curves), and in dibromomethane (black curves).

plasmon band position were determined from Lorentzian fits to the experimental data. Previous work[31] indicated that gold trigonal prisms scatter light far more efficiently than the decahedra; hence, the majority of the particles measured in this work were trigonal prisms, and the discussion reflects this.

The expected surface plasmon shifts were calculated assuming that the surface plasmon resonances of the prisms obey the dipole approximation, so that the peak position is given by

$$\epsilon' = -\frac{1-L}{L} n_{\text{eff}}^{\ 2} \qquad (1)$$

Here ϵ' is the real part of the gold dielectric function. The shape dependent depolarisation factor, L, is unknown. However, the position of the SP band in dibromomethane, which almost index matches to the glass substrate, can be used to determine L for the prisms used here. The observed SP peak wavelengths in CH_2Br_2 ranged from 626 to 629 nm, which corresponds to an average value of $L = 0.177 \pm 0.004$. Having established L, we can predict how the SP band should shift for prisms immersed into different solvents and compare this sensitivity to the observed values for the particles in the same solvents but sitting on the glass substrates.

As a first approximation, we assume that the gold particle experiences an average refractive index given by

$$n_{\text{eff}} = \alpha n_{\text{med}} + (1-\alpha) n_{\text{sub}} \qquad (2)$$

Figure 4 shows the experimental and calculated shifts obtained for each system studied. It is important to stress that these plots were built up by taking a single gold nanocrystal and measuring its spectrum in air and then in a single solvent. It was generally

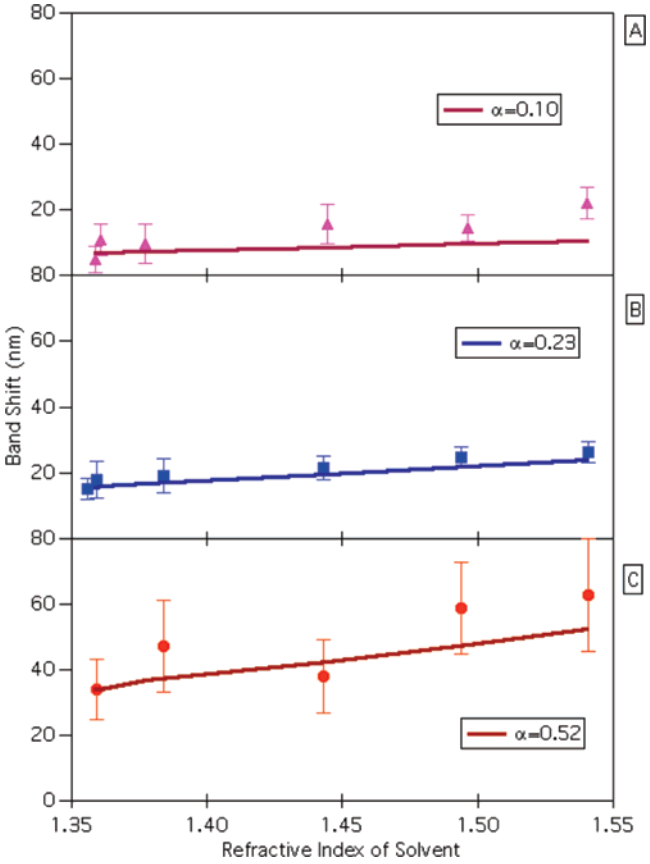

Figure 4. Plots of surface plasmon band shift vs refractive index of solvent for the three systems used (average values, over approximately 30 particles per refractive index), and calculated values: A. Particles immersed in a PVA film, on glass, B. Particles on glass partially immersed in PVA, C. Bare particles on glass. Error bars are the standard deviation of the measurements over approximately 30 particles.

TABLE 1: List of Solvents Used and Respective Refractive Indexes, at 21.8 °C Measured by Abbe Refractometer at 589 nm

solvent	refractive index
acetone	1.359
ethanol	1.361
isopropanol	1.377
chloroform	1.445
toluene	1.496
dibromomethane	1.540

not possible to measure the same particle in multiple solvents because during evaporation of each solvent, residual impurities tended to leave scattering contaminants on the glass slides. Hence a series of single particle measurements were performed in each solvent. In Figure 4A, results for particles completely immersed in a PVA film are shown. The red-shifts observed for the gold particles in air on a glass substrate, ranging from 11 nm for immersion in ethanol to 22 nm for immersion into dibromomethane, are in good agreement with eq 2 if it is assumed that 90% of the particle's surface area is immersed in PVA/glass ($\alpha = 0.10$). Figure 4B shows the shifts obtained for particles partially immersed in PVA, the system most commonly used in single particle experiments. The more pronounced shifts observed, ranging from 18 nm for ethanol to 26 nm for dibromomethane, can be fit well assuming a value of $\alpha = 0.23$, as seen in Figure 4B. The good agreement between these calculations and experiment confirms that both the substrate and the PVA film around the particle alter the effective refractive index of the medium experienced by the gold prisms.

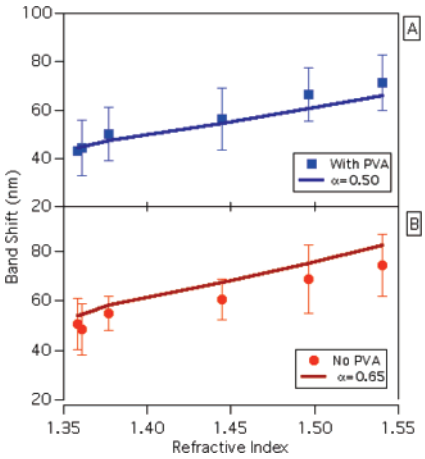

Figure 5. Plot of surface plasmon shifts vs refractive index of the solvent for gold prisms (A) partially immersed in a PVA film and (B) without PVA, on quartz ($n = 1.46$) slides. Error bars are the standard deviation of the measurements over approximately 30 particles.

TABLE 2: Values of α for Gold Nanoprisms on Substrates Exposed to Solvents

system	best α value
NP completely immersed in PVA on glass	0.10
NP partially immersed in PVA on glass	0.23
bare NP on glass	0.52
bare NP on quartz	0.65
NP partially immersed in PVA on fused quartz	0.5

Finally, Figure 4C presents the shifts obtained for bare particles on glass in the absence of PVA. The shifts measured in this case, ranging from 34 nm for ethanol to 63 nm for dibromomethane, are substantially larger than those found when PVA is present, but still significantly smaller than the calculated shifts for a particle in bulk solution, for which we would expect shifts of 102 nm on changing the medium from air to ethanol and 160 nm for air to dibromomethane. The shifts expected from eq 2 with a value of $\alpha = 0.52$ are also plotted in Figure 4C, and this gives good agreement with experiment. This is the key result and indicates that the sensitivity of the surface plasmon band for the triangular prisms on a glass substrate is about half of the dielectric sensitivity in homogeneous solution.

From Figure 4C, it becomes clear that not only the PVA film but also the substrate on its own affects the sensitivity of the SP band to environmental changes. Samples were also prepared employing quartz ($n = 1.46$) as the substrate. The particles used on quartz were slightly larger on average than the ones on glass, and the L measured for these was $L = 0.138 \pm 0.005$. Figure 5 shows results obtained from samples prepared with (A) and without (B) PVA, accompanied by the values calculated for $\alpha = 0.5$ (A) and 0.65 (B), the values that best agree with the experimental results.

Discussion

The results presented here demonstrate that surface plasmon spectroscopy of small metal nanocrystals dispersed on substrates cannot be interpreted unless the microenvironment around the nanocrystals is well-defined. Consequently, the sample preparation method plays a crucial role in terms of the SP sensitivity to the environment. The results here indicate that the surface plasmon band of small trigonal gold prisms deposited onto a clean glass substrate exhibit about half the RI sensitivity that would be observed in bulk media. Codeposition of polymers to fix the particles decreases the sensitivity even further. However, small shifts were observed even for samples containing nanoparticles completely immersed in PVA. To explain this, we must assume that such PVA films are porous and that solvent can permeate through the pores, changing the effective refractive index of the medium. A value of $\alpha = 0.10$ yields good fits to the shifts obtained experimentally, consistent with the presence of pores in the PVA film.

Schatz and colleagues[32,34] have proposed that for small particles the fractional area of the particles exposed to the medium provides a rough guide to the value of alpha. The fraction of nanoparticles in a particular environment (and thus experiencing the refractive index of that medium) is estimated to be about 0.4−0.5 for a trigonal prism, since the larger exposed basal plane of the prism usually constitutes about 0.4−0.5 of the total surface area, depending on the prism thickness. The data here for the particles on bare glass are consistent with that empirical model.

When the same experiments were performed on quartz slides, substantially larger shifts were observed (Figure 5A) than for glass substrates, indicating a larger percentage of the particle surface was exposed to the external medium. Because the refractive indices of the two substrates do not differ greatly, this could only be achieved by the presence of a thinner PVA film. Since the same concentration and spinning speed were used during sample preparation, the only parameter that could be influencing the film thickness is substrate roughness. The mean surface roughness of soda glass microscope slides is around 3.5 nm per square micron,[35] whereas the mean roughness of quartz slides is of about 2 nm[36] per square micron, much smaller than that of glass. It is possible that the PVA films are thicker on the rougher glass slides, since the processed liquid will not spread as quickly during spin coating. Table 2 presents the values of α that best fit each system.

It is clear from these results that surface plasmon spectroscopy of single particles is highly sensitive to the method of sample preparation. Precise and predictable particle films with well-defined SP sensitivity will depend on a number of parameters, such as the roughness and wettability of the substrate, spin coating speed, and polymer viscosity and concentration. The sensitivity will of course be highly dependent on the gold particle shape, which we will consider in detail elsewhere.

Conclusions

The effects of a substrate on the sensitivity of the surface plasmon resonance of a metal particle have been investigated. As observed in previous studies using samples created by nanoparticle lithography,[37] the SP resonance is not as sensitive to the medium when the particle is adsorbed to a substrate. The use of PVA and other polymers to facilitate spin coating and homogeneous distribution of particles on substrates is found to have a substantial and negative influence on the SP sensitivity. Even partial coverage of the particle by polymer reduces the shifts observed during dielectric increases in the environment. Furthermore, surface roughness is also an important parameter since this influences how the polymer film spreads and hence the degree of coverage of the particles during sample preparation for dark field microscopy.

Acknowledgment. C.N. thanks the University of Melbourne for MIRS and MIFRS postgraduate scholarships, and P.M. thanks the ARC for support through the Grants DP 0451651 and FF 01454681. Ana Sánchez-Iglesias is thanked for assistance during synthesis and LMLM thanks the Spanish Ministerio de Educación y Ciencia for funding through grants PCI2005-A7-0075 and MAT2007-62696.

Supporting Information Available: Additional information available as noted in text. This material is available free of charge via the Internet at http://pubs.acs.org.

References and Notes

(1) Miller, M. M.; Lazarides, A. A. *J. Phys. Chem. B* **2005**, *109*, 21556−21565.
(2) Miller, M. M.; Lazarides, A. A. *J. Opt. A* **2006**, *8*, S239−S249.
(3) Templeton, A. C.; Pietron, J. J.; Murray, R. W.; Mulvaney, P. *J. Phys. Chem. B* **2000**, *104*, 564−570.
(4) Underwood, S.; Mulvaney, P. *Langmuir* **1994**, *10*, 3427−3430.
(5) Mulvaney, P. *Langmuir* **1996**, *12*, 788−800.
(6) Novo, C.; Mulvaney, P. *Nano Lett.* **2007**, *7*, 520−524.
(7) Pastoriza-Santos, I.; Gomez, D.; Perez-Juste, J.; Liz-Marzan, L. M.; Mulvaney, P. *Phys. Chem. Chem. Phys.* **2004**, *6*, 5056−5060.
(8) Perez-Juste, J.; Liz-Marzan, L. M.; Carnie, S.; Chan, D. Y. C.; Mulvaney, P. *Adv. Funct. Mater.* **2004**, *14*, 571−579.
(9) El-Sayed, M. A. *Acc. Chem. Res.* **2001**, *34*, 257−264.
(10) Murphy, C. J.; San, T. K.; Gole, A. M.; Orendorff, C. J.; Gao, J. X.; Gou, L.; Hunyadi, S. E.; Li, T. *J. Phys. Chem.* B **2005**, *109*, 13857−13870.
(11) Arbouet, A.; Christofilos, D.; Del Fatti, N.; Vallee, F.; Huntzinger, J. R.; Arnaud, L.; Billaud, P.; Broyer, M. *Phys. Rev. Lett.* **2004**, 93.
(12) Berciaud, S.; Cognet, L.; Tamarat, P.; Lounis, B. *Nano Lett.* **2005**, *5*, 515−518.
(13) Imura, K.; Nagahara, T.; Okamoto, H. *J. Phys. Chem. B* **2004**, *108*, 16344−16347.
(14) Pelton, M.; Liu, M. Z.; Park, S.; Scherer, N. F.; Guyot-Sionnest, P. *Phys. Rev. B* **2006**, 73.
(15) Sonnichsen, C.; Geier, S.; Hecker, N. E.; von Plessen, G.; Feldmann, J.; Ditlbacher, H.; Lamprecht, B.; Krenn, J. R.; Aussenegg, F. R.; Chan, V. Z. H.; Spatz, J. P.; Moller, M. *Appl. Phys. Lett.* **2000**, *77*, 2949−2951.
(16) van Dijk, M. A.; Lippitz, M.; Orrit, M. *Phys. Rev. Lett.* **2005**, 95.
(17) Novo, C.; Gomez, D.; Perez-Juste, J.; Zhang, Z. Y.; Petrova, H.; Reismann, M.; Mulvaney, P.; Hartland, G. V. *Phys. Chem. Chem. Phys.* **2006**, *8*, 3540−3546.
(18) Sonnichsen, C.; Franzl, T.; Wilk, T.; von Plessen, G.; Feldmann, J.; Wilson, O.; Mulvaney, P. *Phys. Rev. Lett.* **2002**, *88*, 077402−077401.
(19) Brolo, A. G.; Gordon, R.; Leathem, B.; Kavanagh, K. L. *Langmuir* **2004**, *20*, 4813−4815.
(20) Larsson, E. M.; Alegret, J.; Kall, M.; Sutherland, D. S. *Nano Lett.* **2007**, *7*, 1256−1263.
(21) Atwater, H.; Maier, S.; Polman, A.; Dionne, J. A.; Sweatlock, L. *MRS Bull.* **2005**, *30*, 385.
(22) Yang, Y.; Xiong, L. M.; Shi, J. L.; Nogami, M. *Nanotechnology* **2006**, *17*, 2670−2674.
(23) Orendorff, C. J.; Gearheart, L.; Jana, N. R.; Murphy, C. J. *Phys. Chem. Chem. Phys.* **2006**, *8*, 165−170.
(24) Emery, S. R.; Haskins, W. E.; Nie, S. M. *J. Am. Chem. Soc.* **1998**, *120*, 8009−8010.
(25) Mock, J. J.; Smith, D. R.; Schultz, S. *Nano Lett.* **2003**, *3*, 485−491.
(26) Curry, A.; Nusz, G.; Chilkoti, A.; Wax, A. *Opt. Express* **2005**, *13*, 2668−2677.
(27) Driskell, J. D.; Lipert, R. J.; Porter, M. D. *J. Phys. Chem. B* **2006**, *110*, 17444−17451.
(28) Pinchuk, A.; Hilger, A.; von Plessen, G.; Kreibig, U. *Nanotechnology* **2004**, *15*, 1890−1896.
(29) Sanchez-Iglesias, A.; Pastoriza-Santos, I.; Perez-Juste, J.; Rodriguez-Gonzalez, B.; de Abajo, F. J. G.; Liz-Marzan, L. M. *Adv. Mater.* **2006**, *18*, 2529−2534.
(30) Harbron, E. J.; Barbara, P. F. *J. Chem. Educ.* **2002**, *79*, 211−213.
(31) Novo, C.; Funston, A. M.; Pastoriza-Santos, I.; Liz-Marzan, L. M.; Mulvaney, P. *Angew. Chem.-Int. Ed.* **2007**, *46*, 3517−3520.
(32) Malinsky, M. D.; Kelly, K. L.; Schatz, G. C.; Van Duyne, R. P. *J. Am. Chem. Soc.* **2001**, *123*, 1471−1482.
(33) Kelly, K. L.; Coronado, E.; Zhao, L. L.; Schatz, G. C. *J. Phys. Chem. B* **2003**, *107*, 668−677.
(34) Sherry, L. J.; Jin, R. C.; Mirkin, C. A.; Schatz, G. C.; Van Duyne, R. P. *Nano Lett.* **2006**, *6*, 2060−2065.
(35) Platypus Technologies, Products Catalogue FAQ. http://www.platypustech.com/goldsubstrates.html (24/07/07).
(36) Structure Probe, Inc., SPI Supplies Brand Quartz Microscope Slides and Cover Slips, in Catalogue. http://www.2spi.com/catalog/ltmic/quartz.shtml#Slides (24/07/07).
(37) Malinsky, M. D.; Kelly, K. L.; Schatz, G. C.; Van Duyne, R. P. *J. Phys. Chem. B* **2001**, *105*, 2343−2350.